Available online at www.sciencedirect.com
SCIENCE DIRECT®
Genomics 84 (2004) 126–138
GENOMICS
www.elsevier.com/locate/ygeno

Polycystin-1L2 is a novel G-protein-binding protein

Takeshi Yuasa,[1] Ayumi Takakura,[1] Bradley M. Denker, Bhuvarahamurthy Venugopal, and Jing Zhou*

Renal Division, Department of Medicine, Brigham and Women's Hospital and Harvard Medical School, Boston, MA 02115, USA

Received 29 September 2003; accepted 12 February 2004

Available online 9 April 2004

Abstract

Mutations in genes encoding polycystin-1 (PC1) and polycystin-2 cause autosomal dominant polycystic kidney disease. The polycystin protein family is composed of Ca^{2+}-permeable pore-forming subunits and receptor-like integral membrane proteins. Here we describe a novel member of the polycystin-1-like subfamily, polycystin-1L2 (PC1L2), encoded by *PKD1L2*, which has various alternative splicing forms with two translation initiation sites. PC1L2 short form starts in exon 12 of the long form. The longest open reading frame of *PKD1L2* short form, determined from human testis cDNA, encodes a 1775-amino-acid protein and 32 exons, whereas the long form is predicted to encode a 2460-residue protein. Both forms have a small receptor for egg jelly domain, a G-protein-coupled receptor proteolytic site, an LH2/PLAT, and 11 putative transmembrane domains, as well as a number of rhodopsin-like G-protein-coupled receptor signatures. RT-PCR analysis shows that the short form, but not the long form, of human *PKD1L2* is expressed in the developing and adult heart and kidney. Furthermore, by GST pull-down assay we observed that PC1L2 and polycystin-1L1 are able to bind to specific G-protein subunits. We also show that PC1 C-terminal cytosolic domain binds to $G\alpha_{12}$, $G\alpha_s$, and $G\alpha_{i1}$, while it weakly interacts with $G\alpha_{i2}$. Our results indicate that both PC1-like molecules may act as G-protein-coupled receptors.

Keywords: ADPKD; Polycystic kidney disease; Polycystin-1L2; PKD1L2; G-protein-coupled receptor

Autosomal dominant polycystic kidney disease (ADPKD) is one of the most common monogenic genetic diseases, with an estimated disease gene frequency of 1:1000, affecting approximately 600,000 individuals and accounting for approximately 4% of all end-stage renal disease in the United States and 8–10% in Europe and Australia [1]. The disease is characterized by progressive development of epithelial-lined cysts in the kidney. Mutations in the *PKD1* and *PKD2* genes are responsible for 85–90 and 10–15% of cases of ADPKD, respectively [1,2]. Polycystin-1 (PC1) and PC2, the respective gene products of *PKD1* and *PKD2*, are considered to be components of a common signaling pathway that regulates renal tubular cell function.

Polycystins are membrane proteins that share significant sequence homology with each other. The polycystin proteins are divided into two subfamilies: the PC1-like subfamily, comprising PC1 [3,4], PCREJ [5], and the recently identified PC1L1 [6], and the PC2-like subfamily, which includes PC2 [7,8], PCL (or 2L or 2L1) [9,10], and PC2L2 [11,12]. The PC2-like subfamily of proteins shares structural homology with cation channels such as those of the transient receptor potential (*Trp*) [9] and the voltage-gated Ca^{2+}, Na^+, and K^+ channel family proteins; it has been recently established that PC2 functions as a cation channel [13–16]. PCL is a Ca^{2+}-modulated nonselective cation channel permeable to Na^+, K^+, and Ca^{2+} ions [17]; its channel activity is modulated by intracellular Ca^{2+} concentration and pH. Conversely, PC1 subfamily proteins are relatively large (>2000 amino acid residues) and have a large extracellular N-terminal domain, followed by 11 transmembrane domains [18] and a relatively short C-terminal cytosolic domain containing a coiled-coil structure known to interact with PC2 [19,20]. It is likely that this subfamily of proteins mediates the transmembrane influx of calcium indirectly, similar to the sea urchin sperm receptor for egg jelly (suREJ) [21]. Indeed, we have recently shown that stimulating PC1 with an antibody or fluid flow activates the PC2 channel [22], and PC1 mutant cells fail to show flow-

* Corresponding author. Fax: (617) 525-5861.
E-mail address: zhou@rics.bwh.harvard.edu (J. Zhou).
[1] These authors contributed equally to this work.

0888-7543/$ - see front matter © 2004 Elsevier Inc. All rights reserved.
doi:10.1016/j.ygeno.2004.02.008

induced Ca^{2+} response [23]. The C-terminus of PC1 has been reported to bind to RGS7, a member of the regulators of G-protein signaling (RGS) family, and to heterotrimeric $G\alpha_{i/o}$ [24,25]. We have found that the functional activation of $G\alpha_{i/o}$ protein by full-length PC1 is independent of RGS protein in sympathetic neurons [22]. PC1 acts as a typical G-protein-coupled receptor (GPCR), modulating voltage-dependent Ca^{2+} channels and G-protein-gated K^+ channels through the activation of $G\alpha_{i/o}$ subunit and the release of $\beta\gamma$ subunits [22]. With JNK/AP1 as a readout for G-protein activation, PC1 appears to activate all four major G-protein families in HEK293T cells [26].

Here we report the identification of a new PC1-like molecule, PC1L2, that is capable of binding to specific G-protein subunits. *PKD1L2* has a long and a short form with respective translation start sites and multiple alternatively spliced variants. Only the short form is expressed in the heart and kidney. Studies on related members of the polycystin family have been instrumental in dissection of the possible roles of the proteins mutated in ADPKD. The investigation of this novel PC1-like protein will lead to a better understanding of the function of PC1.

Results

Isolation and characterization of cDNA for a seventh polycystin, human polycystin-1L2

To understand ADPKD proteins further, we attempted to identify new PKD family genes by database searches. We identified the *Homo sapiens* chromosome 16 clone RP11-303E16 (AC092718) with amino acid sequence similarity to PC2. We carried out 5′ and 3′ rapid amplification of cDNA ends (RACE) using a human testis cDNA library. In addition to *PKD1L2* long form, which was recently described [27], we found a short form of *PKD1L2* (GenBank Accession No. AY371495) (Fig. 1). The translation initia-

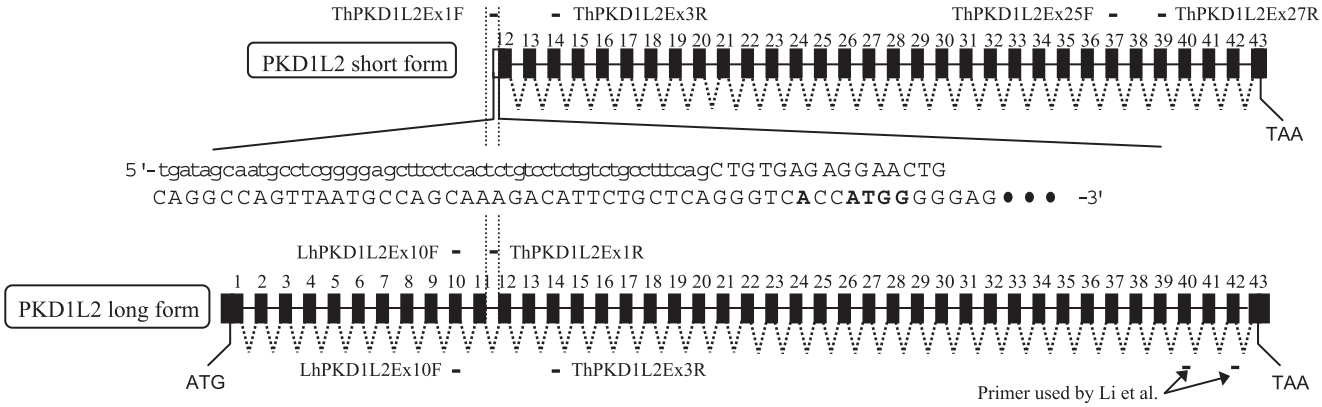

Alternative splicing of human PKD1L2	
Exon (s) skipping	Frame sift
Exon 11	Yes, stop codon at exon 13, truncates the protein by 1805 residues
Exon 21*	No
Exon 27	No
Exon 30	Yes, stop codon at exon 31, truncates the protein by 743 residues
Exon 31*	Yes, stop codon at exon 32, truncates the protein by 734 residues
Exon 30-32	No
Exon 30-32 and 35	No
26 nucleotides in exon 40 (nt 6774-6799) AGGCATCAGCTTCAGTGAGACAGCAG	
Insertion 21 nucleotides in exon 36 (nt 6232-) AATGGCAGTAGCTTTCCCCAG	

*, indicates splicing variants also identified by Li et al. [27]

Fig. 1. Various forms of human *PKD1L2* and the position of primers used for RT-PCR. Top: Human *PKD1L2* short form with 32 exons and a 111-bp 5′-untranslated region including 53 bp in intron 11 (lowercase). Middle: Human *PKD1L2* long form with 43 exons. ThPKD1L2Ex1F and ThPKD1L2Ex1R are located in intron 11. The primer pair ThPKD1L2Ex1F and ThPKD1L2Ex3R can amplify only the *PKD1L2* short form. The primer pair ThPKD1L2Ex25F and ThPKD1L2Ex27R can amplify both short and long forms of *PKD1L2*. The primer pair LhPKD1L2Ex10F and ThPKD1L2Ex1R can amplify neither the short nor the long form. The primer pair LhPKD1L2Ex10F in exon 10 and ThPKD1L2Ex3R in exon 14 is *PKD1L2* long-form-specific. Bottom: Alternative splicing forms of human *PKD1L2*.

tion site for the *PKD1L2* short form, located in exon 12 of the long form, has a G nucleotide following the ATG codon at position +4 and an A nucleotide at position −3, which is in complete agreement with the consensus sequence for a mammalian translation initiation site [28]. By contrast, the translation start site for *PKD1L2* long form (5′-TCAAGC*ATG*AG-3′) is not accompanied by a typical Kozak sequence. In total, the cDNA sequence of the *PKD1L2* short form has 5325 bp and 1775 amino acid residues in the open reading frame and a 111-bp 5′-untranslated region (5′ UTR) including 53 bp in intron 11 of the long form. Furthermore, to determine whether the short form of *PKD1L2* is an alternatively spliced form of the long form, we performed reverse transcriptase-polymerase chain reaction (RT-PCR) using primer pairs located in the 5′ UTR of the short form and the upstream exons of the long form (e.g., ThPKD1L2Ex1R and LhPKD1L2Ex10F) (Table 1 and Fig. 1), which detected no PCR products (data not shown). By contrast, we detected the expected PCR products using a primer located in intron 11 of the long form (the 5′ UTR of the short form) and downstream exons of the long form (e.g., exon 14) (Fig. 1). These data indicate that the *PKD1L2* short form uses a start site different from that of the long form for transcription. We determined the exon/intron structure of the human *PKD1L2* by comparing our cDNA sequences with genomic sequences in GenBank (Table 2).

All our sequences in Table 2, although different from the sequences of Li et al. in multiple positions [27], match the genomic sequence. Our cDNA sequence has 13 nucleotide differences compared to the genomic sequence, one of which does not change the peptide sequence (polymorphisms). Among the remaining 12 changes, 4 are identical, 1 is similar to the sequence of Li et al., and 7 are distinct amino acid substitutions. The sequence of Li et al. has 11 nucleotide differences compared to the genomic sequence. In addition to the 4 changes that are identical, and 1 that is similar to what we observed in this study, there are 6 differences that result in single amino acid substitutions and frameshifts due to a single base pair deletion and a single base pair insertion. These sequence changes are shown in Fig. 2A.

Kyte–Doolittle hydropathy analysis of *PKD1L2* revealed 11 highly hydrophobic regions suggestive of the presence of 11 transmembrane segments. After further analysis using two other transmembrane prediction programs (TMHMM and TMpred) and comparing these results with those obtained for PC1 and PCREJ, we postulated a topology model with 11 transmembrane segments for PC1L2. Analysis with the protein second-structure prediction programs SMART and Pfam revealed a small REJ domain, a GPS domain, and an LH2/PLAT domain, all of which are also found in PC1, as well as an ion transporter domain similar to one found in PC2 (Figs. 2A and 2B). Interestingly, PC1L2 has a number of rhodopsin-like GPCR superfamily signatures throughout the sequence, similar to those found in PC1, PCREJ, and PC1L1. Phylogenetic analysis of human *PKD1L2* with the other polycystins shows that *PKD1L2* belongs to the PC1-like subfamily (Fig. 3).

To examine the alternative splicing variants, we performed RT-PCR using various primer pairs (Table 1). The multiple bands obtained by the RT-PCR were sequenced. We found some nucleotide insertions and a number of exon-

Table 1
Primer sequences of human *PKD1L2* used in this study

Name	Sequence (5′–3′)	Position (exon)
hP7F1	GGTTGGCAGTGCCCAGATTCG	36
hP7F2	AGGGTCCGGGAAAGCTCTTGC	36
hP7F3	TGGTATTTGGACAACACCCCAACAG	12
hP7F4	AGAACTGCGGAGCCTCCGGCTGTG	26
hP7R1	CTCTAGCGTCAGCGTGACAATG	37
hP7R2	AGACAGTGAACTCCACAAACAC	37
hP7R3	AGTATCCTCCTCATCGTCCACTCTCTTC	33
hP7R4	GACCAGCACCCGGCTCACATACCACG	26 and 27
hP7R5	CTCCTCTGGGGCAATAGTGCAGGCA	14
hP7R6	TCTCACAGCTGAAAGGCAGACAGAGGAC	12[a]
LhPKD1L2EX10F	TACATCCAACCTGGTCCATAT	10
ThPKD1L2EX1R	GACAGAGGACAGAGTGAGGAA	[b]
ThPKD1L2EX1F	GAGCTTCCTCACTCTGTCCTC	[b]
ThPKD1L2EX3R	AGGCACAGTGCTGATCACATA	14
ThPkd1L2Ex25F	TCCGCTATCTCTTTGACAACA	37
ThPkd1L2Ex27R	AGGACAGCCCTC TTCACAAAC	39
hGAPDH/F	AAGGCTGAGAACGGGAAGCTT	
hGAPDH/R	GCCAGTGAGCTTCCCGTTCA	

[a] Intron 11 and exon 12.
[b] Intron 11.

Table 2
Exon/intron structure of human *PKD1L2*

Exon	Size (bp)	3′ Splicing site (acceptor)		5′ Splicing site (donor)	
		This study	Sequence by Li et al.	This study	Sequence by Li et al.
1	301	AGCATGA	ATG	CGGAGGgtaggt	CGGAGGgtaggt
2	162	ttccagGGCCGG	ttccagGGCCGG	AGTTCCgtgagt	AGTTCCgtgagt
3	186	cctcagGGGTTG	cctcagGGGTTG	TGGCAGgtaggg	TGGCAGgtaggg
4	111	tcccagGCCAGT	tcccagGCCAGT	GGGAAGgtgagt	GGGAAGgtgagt
5	148	ccacagCCCTGC	ccacagCCCTGC	ACCGAGgtaaga	ACCGAGgtaaga
6	231	cggcagTGTGTC	cggcagTGTGTC	ATGGAGgtcagt	ATGGAGgtcagt
7	405	acttagGAACAG	acttagGAACAG	TTGAAGgtacat	TTGAAGgtacat
8	78	ttgcagGCACCT	ttgcagGCACCT	TCACAGgcaagg	TCACAGgcaagg
9	50	tcacagCCCCTT	tcacagCCCCTT	AAGAGTgtgagt	AAGAGTgtgagt
10	118	ttgcagAAAGAT	ttgcagAAAGAT	CAT**GTG**gtaggt	CATTGTgtaggt
11	208	tctcagGGTCTT	tctcagGGTCTT	AGTCAGgtgggg	AGTCAGgtgggg
12	121	tttcagCTGTGA	tttcagCTGTGA	GAGCAGgtgagc	GAGCAGgtgagc
13	142	tttcagGCTGAG	tttcagGCTGAG	CCACAGgtgcga	CCACAGgtgcga
14	177	tcccagCACTGA	tcccagCACTGA	AATCAGgtaccg	AATCAGgtaccg
15	146	tgccagGTTCCT	tgccagGTTCCT	GCTAAGgtaggt	GCTAAGgtaggt
16	195	taacagGTGGCA	taacagGTGGCA	CAGAAGgtaccc	CAGAAGgtaccc
17	132	gccaagGTCAGA	gccaagGTCAGA	GCCCAGgtgagt	GCCCA**A**Ggtgagt
18	183	acccagTGGGAG	acccagTGGGAG	AGCCAGgtgggt	AGCCAGgtgggt
19	125	tttcagATTGCC	tttcagATTGCC	AAACAGgtacaa	AAACAGgtacaa
20	127	ggccagAATACA	ggccagAATACA	ATAAAGgtaata	ATAAAGgtaata
21	132	tttcagATCATG	tttcagATCATG	ATCGAGgtagaa	ATCGAGgtagaa
22	223	tcacagATCCTG	tcacagATCCTG	CTCCAGgtaggc	CTCCAGgtaggc
23	194	ctacagATGAGC	ctacagATGAGC	TGCCAGgtaagg	TGCCAGgtaagg
24	231	ttgtagGTGGGG	ttgtagGTGGGG	GCCAAGgtgagg	GCCAAGgtgagg
25	102	cttcagGTGAAG	cttcagGTGAAG	TCAAAGgtacct	TCAAAGgtacct
26	179	tttcagGTGACT	tttcagGTGACT	ATCGTGgtgagt	ATCGTGgtgagt
27	147	ctccagGTATGT	ctccagGTATGT	ATTCAGgtactt	ATTCAGgtactt
28	200	ctgcagCCACCT	ctgcagCCACCT	ACTTGGgtaatt	ACTTGGgtaatt
29	218	ccccagGTAAAA	ccccagGTAAAA	**ACCAAGgcaggt**	CCCCAGgtaaaa
30	217	caccagGATGTG	caccagGATGTG	TGAAAGgtaagc	TGAAAGgtaagc
31	229	ctccag**AG**AAAT	ctccagAAATCA	TGCCAGgtaatc	TGCCAGgtaatc
32	205	ttgcagCGCTCT	ttgcagCGCTCT	CTGAAGgtcagg	CTGAAGgtcagg
33	97	tttcagGTGCTG	tttcagGTGCTG	GCCCAGgtaatg	GCCCAGgtaatg
34	138	ccacagACCCCT	ccacagACCCCT	TCCTGGgtaggc	TCCTGGgtaggc
35	186	ccccagCATACT	ccccagCATACT	**CCCCAGgtaagt**	AGGTAAgtcctg
36	306	ttttagGCTTTA	ttttagGCTTTA	GTCAAGgtaagg	GTCAAGgtaagg
37	134	ctgcagAATTCT	ctgcagAATTCT	CTCTGGgtgggc	CTCTGGgtgggc
38	128	ccccagGCACCT	ccccagGCACCT	GTGCAGgtaagg	GTGCAGgtaagg
39	161	**ttccagGGCAAG**	ctggagCTGGCC	GGAGGAgtcagt	GGAGGAgtcagt
40	211	ccacagAGGCAT	ccacagAGGCAT	**ATCGCGgtaagt**	TTCCTGgtactc
41	102	tgacagTCAAAC	tgacagTCAAAC	GAGGAGgtaacg	GAGGAGgtaacg
42	132	tgacagGTCCTG	tgacagGTCCTG	TATCAGgtgagt	TATCAGgtgagt
43	162	ttgcagCTGTCG	ttgcagCTGTCG	GACTAA	GACTAA

Bold letters indicate sequences that are identical to the genomic sequence, but differ from those reported by Li et al. [27]. Lower case letters, intron sequence; upper case letters, exonic sequence.

skipping events; some resulted in frameshift, while others did not (Fig. 1). Alternative transcripts skipping exons 21 and 32 were also reported by Li et al. [27].

Tissue-specific expression of human PKD1L2

We first analyzed the tissue expression pattern of human *PKD1L2* by Northern blot. However, it was not detected by Northern blot analysis of multiple tissues (data not shown). We then examined the expression of human *PKD1L2* by dot-blot analysis using the same cDNA probes containing exons 26 to 37, which detected moderate levels of *PKD1L2* expression in adult and fetal heart, in mammary gland, and in brain, as well as a low level of expression in testis, although the testis cDNA library was initially used to clone this gene (Figs. 4A and 4C). The tissue distribution of *PKD1L2* is similar to that of *PKD1L1* (Figs. 4A and 4B), although the expression of *PKD1L2* in testis was very low compared with *PKD1L1*.

To explore the significance of the short and long forms of *PKD1L2*, we examined the expression pattern of *PKD1L2* by RT-PCR. When using primer pair LhPKD1L2Ex10F and TPKD1L2Ex3R shown in Table 1 and Fig. 1, which does not recognize *PKD1L2* short form, we detected *PKD1L2*

long form in brain and testis. By contrast, we could amplify human *PKD1L2* cDNA in heart, brain, kidney, and testis tissues by one round of PCR using the primer pair ThPKD1L2Ex1F and ThPKD1L2Ex3R, which is specific for *PKD1L2* short form (Fig. 4D). In addition, we could detect PCR fragments containing exons 37 to 39 of human *PKD1L2* in heart, brain, kidney, and testis tissues, consistent with a previous report [27]. Thus, only the short form, not the long form, of *PKD1L2* is expressed in the kidney and heart.

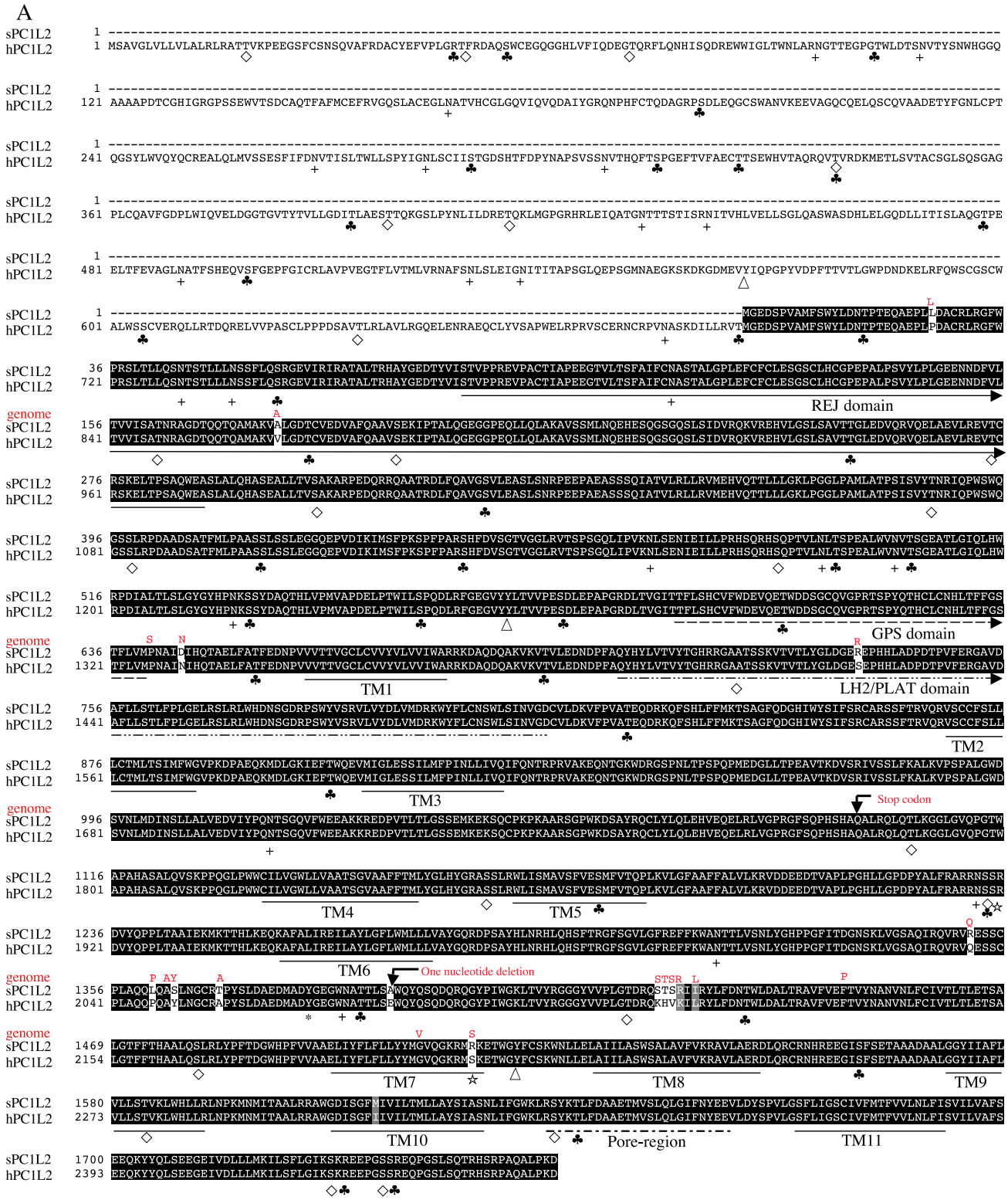

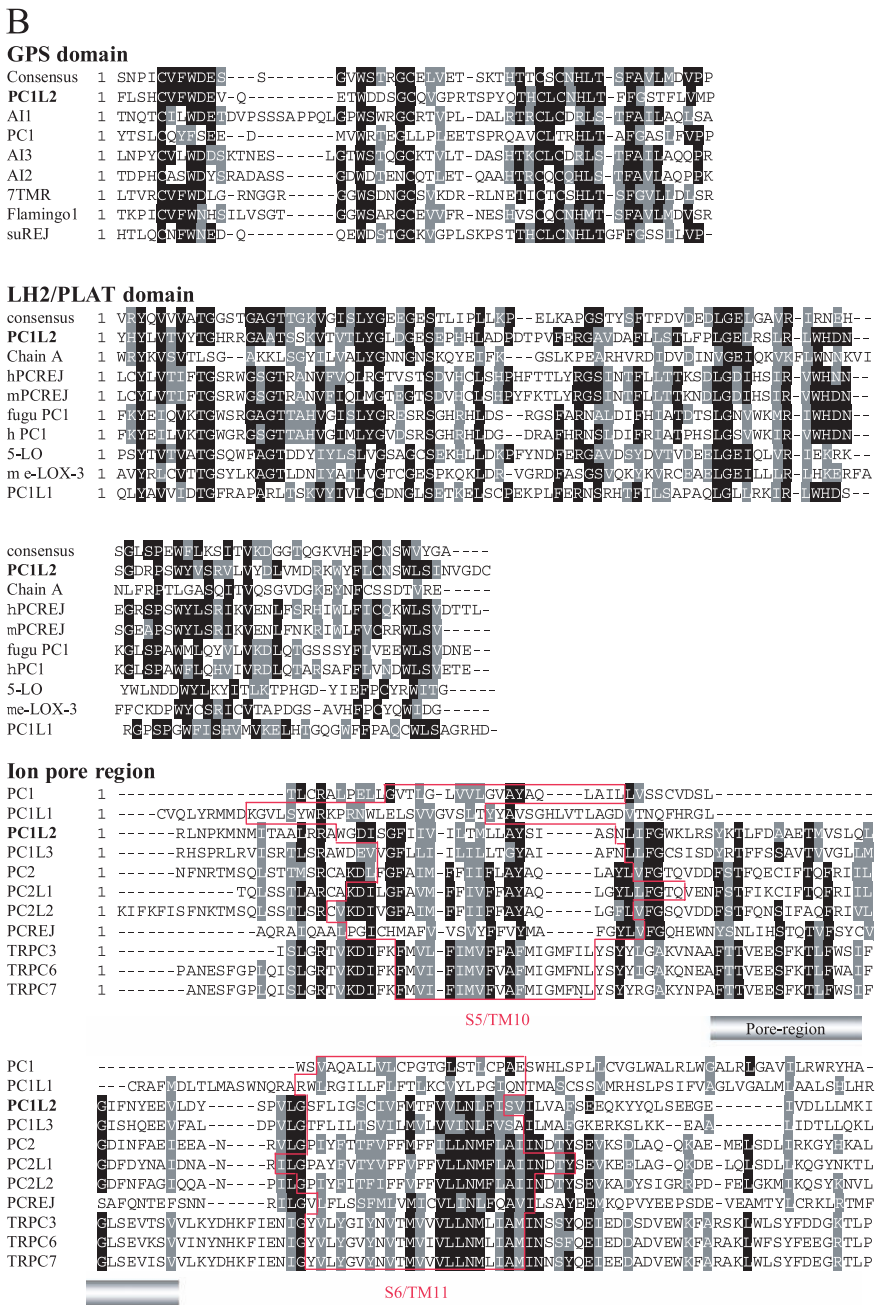

Fig. 2. (A) Alignment of amino acid sequences of human *PKD1L2* short and long forms. Various domains are underlined. Potential N-glycosylation sites are marked with a plus (+). Potential tyrosine-sulfation site is marked with an asterisk (∗). Potential phosphorylation sites are marked as follows: (☆) cAMP phosphorylation sites; (◇) PKC phosphorylation sites; (♣) casein kinase II phosphorylation sites; (△) tyrosine kinase phosphorylation sites. sPC1L2, short form of PKD1L2; hPC1L2, long form of PKD1L2. The sequences identical between the short and the long forms of PC1L2 are shaded in black. Interruptions illustrate the sequences that are different between this study (sPC1L2 line) and that of Li et al. (hPC1L2 line). Genome line shows the genomic sequences (in red) that differ from sPC1L2, hPC1L2, or both. TM, transmembrane. (B) Sequence alignment of GPS and PLAT/LH2 domains and ion pore region. GPS and PLAT/LH2 domains are conserved in PC1 homologs. The ion pore region located between the last two transmembrane domains is conserved in PC2 homologs, PC1L2, and PC1L3. Black and gray shading indicate amino acid identities and similarities, respectively. AI1, AI2, and AI3, brain-specific angiogenesis inhibitor 1, 2, and 3 precursor, respectively; 7TMR, seven-transmembrane-domain receptor; Flamingo1, cadherin EGF LAG seven-pass G-type receptor 2 precursor; Chain A, rat pancreatic lipase-related protein 2; 5-LO, arachidonate 5-lipoxygenase; me-LOX-3, epidermis-type lipoxygenase 3 (mouse).

PC1L2 and PC1L1 may function as a GPCR

We and others have previously shown that PC1 binds to and activates heterotrimeric G-proteins [22,25,26]. To determine whether PC1L2 and PC1L1 may function as a GPCR, we compared their ability to bind to G-proteins with that of PC1. We generated various GST–PC fusion proteins and expressed them in *Escherichia coli* DH5α cells. Various constructs used to produce GST–PC fusion proteins are shown in Fig. 5A. The purified fusion

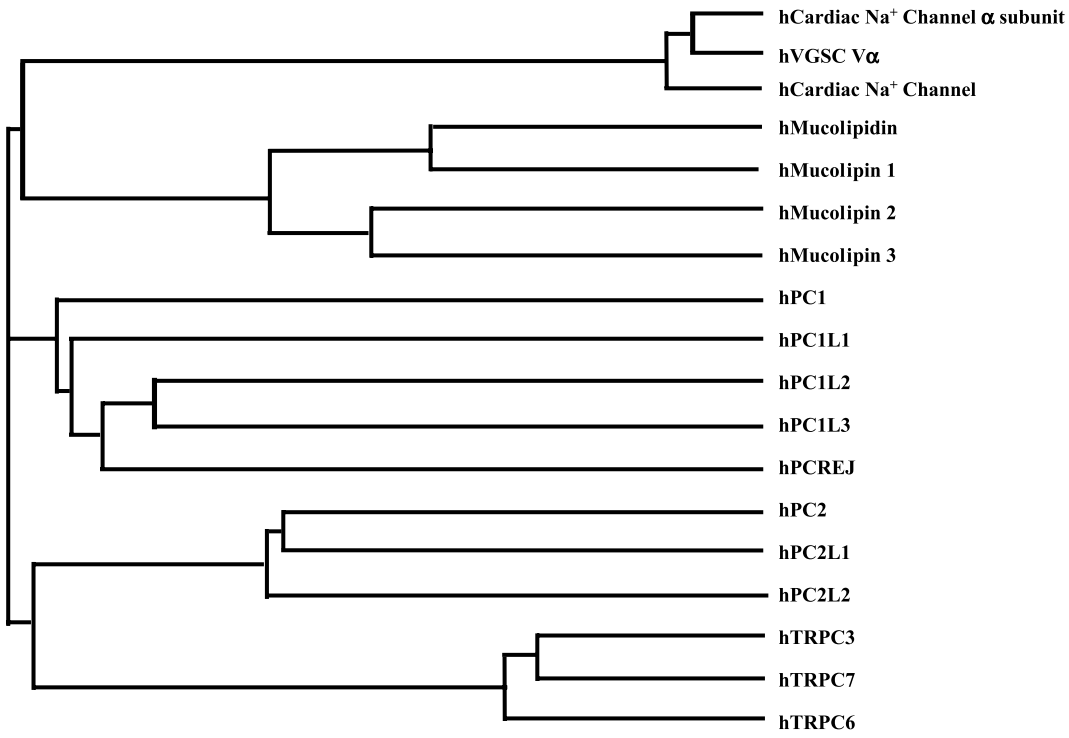

Fig. 3. Phylogenetic relationships between polycystin family and other homologous proteins. The corresponding GenBank accession numbers are cardiac Na^+ channel α subunit, AAO91669; cardiac muscle α subunit, Q14524; voltage-gated Na^+ channel type V α subunit jejunal variant, AAK74065; mucolipidin, CAC07813; mucolipin 1, AAG42242; mucolipin 2, AAM08926; mucolipin 3, NP_060768; TRPC3, transient receptor potential channel 3, NP_003296; TRPC6, transient receptor potential channel 6, NP_004612; TRPC7, short transient receptor potential channel 7, CAD19069.

proteins were confirmed by Western blot using a GST antibody (Fig. 5B). We compared the relative binding of specific G-protein α subunits found in MDCK cells to that of the GST–PC fusion proteins shown in Fig. 5. We calculated the fraction of G-protein bound to the GST fusion protein constructs using the formula [total bound/(total bound + total unbound)]. The PC1 C-terminal cytosolic domain containing the G-protein binding motif binds similarly to both wild-type and constitutively active $G\alpha_{12}$ (Q229L) expressed in MDCK cells (cells described in Meyer et al. [29]) (Fig. 6A) and also interacts with $G\alpha_s$. While the PC1L2 C-terminal cytosolic domain had little detectable binding to $G\alpha_{12}$ or $G\alpha_{i2}$, it interacted relatively well with $G\alpha_S$ and $G\alpha_{i1}$ found in MDCK cell lysates (Fig. 6). GST alone and PC1 first intracellular loop, which does not have a putative G-protein binding motif, were used as negative controls, and as expected, they failed to bind to any G-proteins. We recently identified *PKD1L1* as a sixth member of the PKD family [6]. Although PC1L1 closely resembles PC1 and has a putative G-protein binding motif in the first intracellular loop, there is no knowledge of its function. We found that the first intracellular loop of PC1L1 binds to $G\alpha_{12}$, $G\alpha_s$, and $G\alpha_{i2}$ while its C-terminal cytosolic domain, which does not have G-protein binding domain, binds to $G\alpha_{i1}$ and $G\alpha_{i2}$ (Figs. 6A and 6B). Interestingly, the PC1L1 loop appears to interact better with the constitutively activated $G\alpha_{12}$ (Q229L) subunit than with wild-type $G\alpha_{12}$ (Figs. 6A and 6C). This is in contrast to the PC1 loop, which showed no detectable interactions with either wild-type or $G\alpha_{12}$ (Q229L) subunits. Taken together, these data suggest that, like PC1, both PC1L2 and PC1L1 may function as a GPCR.

Discussion

A new polycystin-1-like molecule, polycystin-1L2

Here we report the identification of a novel PC1-like molecule, PC1L2, in humans. This protein has a small REJ domain, a GPS domain, an LH2/PLAT domain, and 11 transmembrane domains. The REJ domain of this novel protein is homologous to the suREJ domain and is also found in the extracellular domains of PC1, PCREJ, and PC1L1. In all homologous GPCRs, the GPS domain is found in the extracellular portion of the receptors, immediately adjacent to the first transmembrane segment. The GPS is believed to be defined by a highly conserved pattern of Cys residues and a Leu–Thr site that was initially identified in a sperm receptor for egg jelly in sea urchins (suREJ) [30]. While latrophilins and other members of the secretin family are known to be cleaved at the consensus GPS domain, the recent demonstration that suREJ3, and perhaps PC1, is also cleaved at this site [30,31] suggests that PC1-like proteins may also be cleaved. Whether PCREJ, PC1L1,

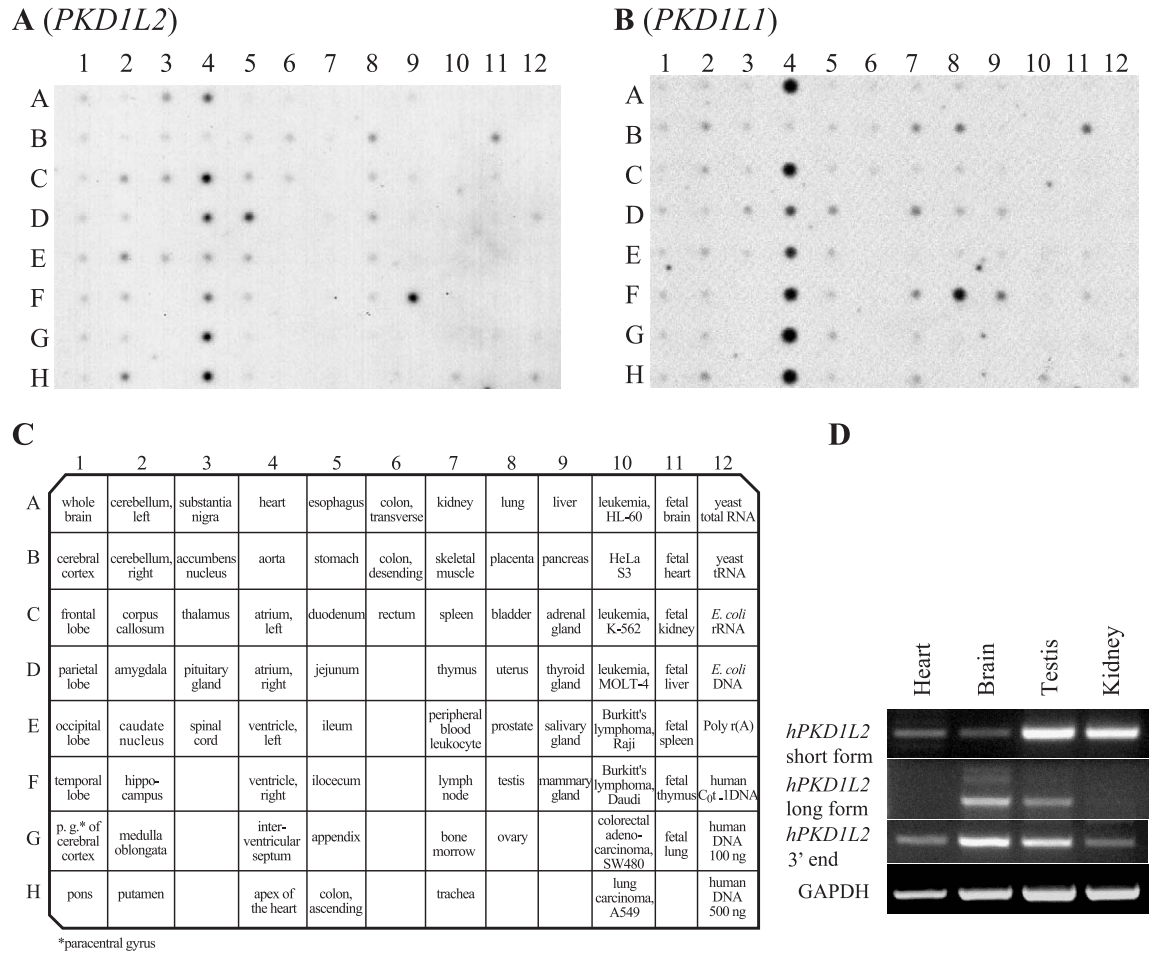

	1	2	3	4	5	6	7	8	9	10	11	12
A	whole brain	cerebellum, left	substantia nigra	heart	esophagus	colon, transverse	kidney	lung	liver	leukemia, HL-60	fetal brain	yeast total RNA
B	cerebral cortex	cerebellum, right	accumbens nucleus	aorta	stomach	colon, desending	skeletal muscle	placenta	pancreas	HeLa S3	fetal heart	yeast tRNA
C	frontal lobe	corpus callosum	thalamus	atrium, left	duodenum	rectum	spleen	bladder	adrenal gland	leukemia, K-562	fetal kidney	*E. coli* rRNA
D	parietal lobe	amygdala	pituitary gland	atrium, right	jejunum		thymus	uterus	thyroid gland	leukemia, MOLT-4	fetal liver	*E. coli* DNA
E	occipital lobe	caudate nucleus	spinal cord	ventricle, left	ileum		peripheral blood leukocyte	prostate	salivary gland	Burkitt's lymphoma, Raji	fetal spleen	Poly r(A)
F	temporal lobe	hippo-campus		ventricle, right	ilocecum		lymph node	testis	mammary gland	Burkitt's lymphoma, Daudi	fetal thymus	human C_0t -1DNA
G	p. g.* of cerebral cortex	medulla oblongata		inter-ventricular septum	appendix		bone morrow	ovary		colorectal adeno-carcinoma, SW480	fetal lung	human DNA 100 ng
H	pons	putamen		apex of the heart	colon, ascending		trachea			lung carcinoma, A549		human DNA 500 ng

*paracentral gyrus

Fig. 4. Expression of the *PKD1L2* gene. (A) Human RNA dot-blot analysis using the 2.1-kb fragment containing exons 26 to 37 of *PKD1L2* as a probe. (B) Human RNA dot-blot analysis using the 3′ 1.9 kb of human *PKD1L1* coding sequence as a probe. (C) Sample positions in the human RNA dot-blot membrane. (D) RT-PCR analysis of human fetal and adult tissues. *PKD1L2* short-form-specific primer pairs and the primer pairs from exons 37 and 39 could PCR amplify adult heart, brain, testis, and fetal kidney cDNA. *PKD1L2* long-form-specific primers pairs could amplify adult brain and testis cDNA. GAPDH-specific primers were used as a positive control.

and PC1L2 are actually cleaved at the GPS site remains to be determined. The GPS domains of several genes are shown in Fig. 2B.

The LH2/PLAT domain is located in the intracellular region between the first and the second transmembrane regions of PC1L2 and contains a β-barrel LH2 domain homologous to a noncatalytic domain of lipoxygenases. Many lipoprotein lipase family proteins possess the LH2/PLAT domain (Fig. 2B). Mutations in some lipases leading to human disease highlight the possible importance of the PLAT domain. Mutations in lipoprotein lipase lead to chylomicronemia, and mutations in triacylglycerol lipase lead to hepatic lipase deficiency [32]. It has been suggested that the PLAT domain is involved in protein–protein and protein–lipid interactions [33]. The presence of the PLAT domain in the first intracellular loop of PC1L1 suggests that it interacts with another membrane protein(s) or lipids.

The GPS domain and LH2/PLAT domains are common to all members of the PC1-like subfamily. However, unlike PC1 and PC1L1, PCREJ and PC1L2 have an ion transport domain but not a coiled-coil domain. Thus, the PC1-like subfamily could be further divided into two groups according to their domain structure: the PC1 subfamily comprising PC1 and PC1L1 and the PCREJ subfamily comprising PCREJ, PC1L2, and PC1L3 (Figs. 2B and 3).

Polycystin-1L2 has several putative phosphorylation sites: 27 protein kinase C phosphorylation sites, 38 casein kinase phosphorylation sites, 2 cAMP phosphorylation sites, and 3 tyrosine kinase phosphorylation sites with strong motif sequences (Fig. 2A). Phosphorylation of these motif sequences may be involved in the regulation of downstream signaling mediated by PC1L2. PC1L2 also has 23 N-glycosylation sites and a tyrosine sulfation site.

Polycystin-1L2 binds to selected G-protein subunits

Of the Gα subunits tested, PC1L2 preferentially interacted with $G\alpha_s$ and $G\alpha_{i1}$ subunits and did not interact with

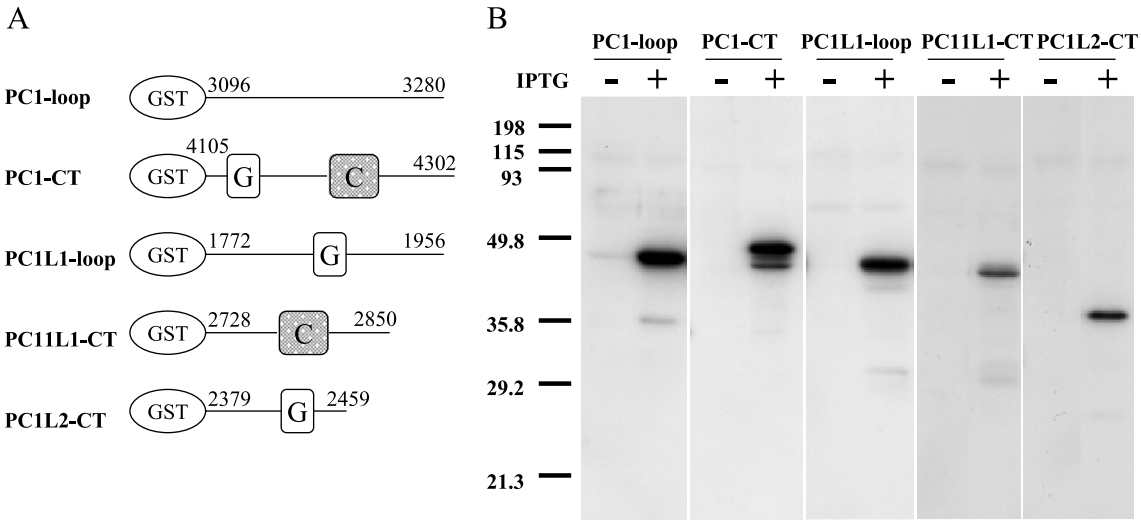

Fig. 5. Generation of GST–polycystin fusion proteins. (A) The GST–polycystin fusion protein constructs used for the binding assay. G-protein binding motif is indicated by the box labeled G. Coiled-coil domain is indicated by hatched box labeled C. PC1-loop, the first intracellular loop (residues 3096–3280) of PC1; PC1-CT, the C-terminal cytosolic domain (residues 4105–4302) of PC1; PC1L1-loop, the first intracellular loop (residues 1772–1956) of PC1L1; PC1L1-CT, the C-terminal cytosolic domain (residues 2728–2850) of PC1L1; PC1L2-CT, the C-terminal cytosolic domain (residues 2379–2459) of PC1L2. (B) Western blot analysis of the GST–polycystin fusion proteins. Purified GST–polycystin fusion proteins were electrophoresed and blotted with a GST antibody. PC1-loop, PC1-CT, PC1L1-loop, and PC1L1-CT were induced with 0.1 mM IPTG, PC1L2-CT was induced with 1 mM IPTG.

$G\alpha_{12}$. This is in contrast to the PC1 and PC1L1 domains, which interacted with $G\alpha_{12}$, $G\alpha_s$, and $G\alpha_{i2}$. Although these experiments are not quantitative, they do suggest discrimination of PC1, PC1L1, and PC1L2 for different Gα subunits. For example, PC1L2 C-terminal domain interacts with $G\alpha_{i1}$ but not with $G\alpha_{i2}$, even though these two Gα subunits are over 90% identical. In addition, both PC1 and PC1L1 interact with $G\alpha_{12}$, while PC1L2 has almost no detectable interactions. Notably, the PC1L1 loop appeared to prefer the active conformation of $G\alpha_{12}$ (Q229L), while there was little difference for the PC1 C-terminal domain and no detectable interactions with either conformation of $G\alpha_{12}$ for the PC1L1 C-terminal domain. The common interacting Gα subunit for all three proteins (PC1, PC1L1, and PC1L2) was $G\alpha_s$. This observation may reflect the relative importance of $G\alpha_s$ regulation of adenylyl cyclase in cystic diseases.

$G\alpha_s$ is abundantly expressed in the kidney, it activates adenylyl cyclase and increases cAMP, while $G\alpha_i$ decreases the level of cAMP. Cystogenesis in ADPKD is thought to involve increased cell proliferation and fluid secretion, both of which are stimulated by cAMP. In addition, recent evidence has shown that ADPKD cells have an altered response to cAMP. Cyclic AMP inhibits proliferation of normal kidney cells but stimulates ADPKD cells to proliferate [34–36]. Thus, abnormal PC1-, PC1L1-, and PC1L2-mediated $G\alpha_s$ signaling may be a direct cause of the increase in intracellular cAMP concentrations in cysts of ADPKD kidneys.

In addition to the kidney, PC1L2 is expressed in fetal and adult heart (particularly in myocytes, data not shown), mammary glands, and testis. Of note, $G\alpha_{i2}$, $G\alpha_{i3}$, and $G\alpha_s$, but not $G\alpha_{i1}$, are also expressed in the left ventricle [37]. It is thus possible that PC1L2 plays a role in normal cardiac development and function. Hypertension, heart valve defects, and cerebral and aortic aneurysms are also complications of ADPKD. Left ventricular hypertrophy often occurs very early in the course of this condition even in normotensive patients [38]. It will be interesting to see whether mutations in *PKD1L2* result in any cardiac phenotypes.

Only very weak expression of *PKD1L2* was found in the testicular interstitial cells, in contrast to the abundant expression of *PKD1L1* and *Pkd1L1* in the Leydig cells. It has previously been suggested that an association exists between epididymal, seminal vesicle, and prostatic cysts and male infertility in ADPKD [39], and it is tempting to speculate that *PKD1L1* and *PKD1L2* may play a role in this regard.

Polycystin channels

While the PC2 subfamily proteins function as calcium-permeable nonselective cation channels [13–17], the PC1 subfamily proteins are likely ion channel regulators [22]. We did not detect channel activity when we overexpressed PC1 [22], consistent with another study [40] and the lack of a pore region in PC1 (Fig. 2B). However, it would be interesting to see whether PC1L2 and/or PC1L3 can function as an ion channel since they do have a pore region (Fig. 2B). Although there is no evidence that PC1 and related molecules are able to form a pore, we show here that both PC1L1 and PC1L2, like PC1, can bind to specific Gα subunits; thus, they are likely to act as GPCRs in cells and tissues in which they are expressed.

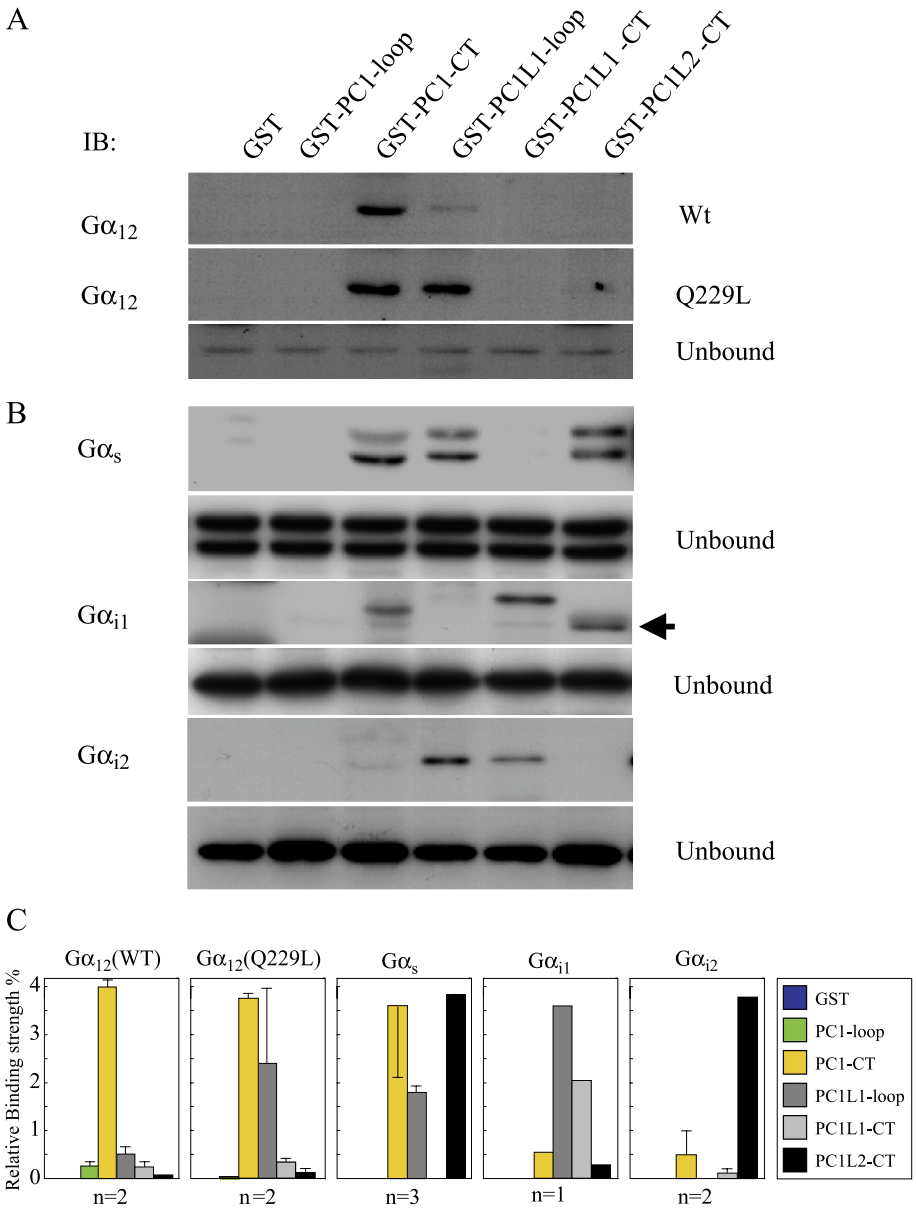

Fig. 6. G-protein pull-down assay. GST–polycystin fusion proteins and GST alone fixed on beads were incubated with various cell lysates. (A) Wild-type (Wt) or constitutively active $G\alpha_{12}$ (Q229L)-expressing MDCK cell lysates were used for binding to $G\alpha_{12}$. (B) Untransfected MDCK cell lysates were used for binding to $G\alpha_s$, $G\alpha_{i1}$, or $G\alpha_{i2}$. The bound proteins were eluted and analyzed by Western blot with antibodies to indicated G-protein subunits. Unbound fraction was loaded as a control. IB, immunoblot. Arrow shows the expected size for $G\alpha_{i1}$. (C) Percentage of total Gα subunit bound to GST–polycystin fusion proteins. Band intensity was determined from scanned images using NIH Image 1.62 software and total amounts of Gα in bound and unbound fractions were calculated. The percentage bound was determined from the formula [total bound/(total bound + total unbound)].

A candidate gene for polycystic kidney disease or other diseases

The expression of *PKD1L2* in the kidney makes it a candidate genetic modifier for ADPKD and a candidate gene for other unmapped cystic kidney diseases. In addition, its location on chromosome 16q24 (determined by FISH mapping, data not shown) suggests that it is a positional candidate gene for several mapped human genetic disorders for which genes have not been cloned, such as Wilms tumor [41] and dehydrated hereditary stomatocytosis (DHS) [42], both involving genes located on chromosome 16q24. The red blood cells in DHS have a membrane abnormality with increased permeability to cations, resulting in a greater efflux of K^+ than of Na^+, which leads to a well-compensated hemolytic anemia. The long arm of chromosome 16 is also a target for loss of heterozygosity in several malignant tumors, such as breast [43], prostate [44], lung [45], and hepatocellular [46] cancers as well as pediatric rhabdomyosarcoma [47], suggesting that 16q harbors a multitumor-suppressor gene. As the mechanisms of cystogenesis in PKD are

analogous to tumorigenesis, it is possible that *PKD1L2* is a candidate gene for one of these particular genetic diseases. Further investigation is necessary to clarify the potential relationship between *PKD1L2* and these genetic disorders.

Materials and methods

Isolation of human PKD1L2

BLAST analysis of the GenBank databases with human *PKD2* revealed significant hits with the *H. sapiens* chromosome 16 clone RP11-303E16 (AC092718). Primers specific to the putative exonic sequence in clone RP11-303E16 were used to perform RT-PCR on human testis cDNA. The primers used in this study are shown in Table 1. We performed 5′ and 3′ RACE on Marathon-Ready cDNA of human testis (Clontech). AdvanTaq DNA polymerase (Clontech) was used to perform touchdown PCR with cycling parameters as follows: initial denaturation at 94°C for 2 min, 5 cycles at 94°C for 30 s and at 72°C for 4 min, 5 cycles at 94°C for 30 s and at 70°C for 4 min, 30 cycles at 94°C for 30 s and at 68°C for 4 min, and a final extension at 68°C for 7 min. For 5′ RACE, primers AP1 [5′-CCATCCTAATACGACTCACTATAGGGC-3′ (Clontech)] and hP7R1 were used to perform the first PCR. Nested PCR for 5′ RACE was performed using 1 μl of the diluted first PCR product (1:100) and the nested primers AP2 [5′-ACTCACTATAGGGCTCGAGCGGC-3′ (Clontech)] and hP7R2. For the second 5′ RACE, primers AP1 and hP7R3 were used to perform the first PCR. The second nested PCR for 5′ RACE was performed with the nested primers AP2 and hP7R4. We performed the third 5′ RACE to confirm the 5′ cDNA end with the primer sets AP1 and hP7R5 and AP2 and hP7R6. 3′ RACE amplification was similarly carried out with AP1 and hP7F1 as the first PCR primer set and AP2 and hP7F2 as the nested primer set. Prominent bands were excised from the agarose gel, purified, and sequenced. The sequences obtained were compared with the sequence data of the clone RP11-303E16.

Sequence analysis

DNA sequences obtained by 5′ RACE and 3′ RACE were aligned to give an overall consensus sequence. Alignment analysis was performed using ClustalW (http://clustalw.genome.ad.jp/) and boxshade3.21 (http://www.ch.embnet.org/software/BOX_form.html). Motif (http://motif.genome.ad.jp/), Smart (Simple Modular Architecture Research Tool) (http://smart.embl-heidelberg.de/), and Pfam (Protein Families Database) (http://www.sanger.ac.uk/Software/Pfam/search.shtml) programs were used to predict the protein function and localization. The TMHMM (http://genome.cbs.dtu.dk/services/TMHMM/) and TMpred (Prediction of Transmembrane Regions and Orientation) (http://www.ch.embnet.org/software/TMPRED_form.html) programs were used to predict the transmembrane helices. Prediction of coiled-coil structure by Lupas algorithm was performed using Coils (http://www.ch.embnet.org/software/COILS_form.html). The phylogenetic trees were plotted using TreeView [48].

RNA dot-blot and Northern blot hybridization

Human Multiple Tissue Array (Clontech) and Multiple Tissue Northern Blot (Clontech) were hybridized with a randomly labeled 2.1-kb coding sequence of human *PKD1L2,* which was amplified by RT-PCR using hP7F4 and hP7R1 in ExpressHyb hybridization solution (Clontech) at 50°C overnight, as previously described [9]. The radiolabeled membranes were washed twice in 2× SSC, 0.05% SDS at 50°C and twice in 0.1× SSC, 0.1% SDS at 50°C. Signals were visualized by autoradiography.

Reverse transcription-polymerase chain reaction

The first-strand cDNA was synthesized from 5 μg of the total RNA from human heart (kind gift from Dr. Yasuda, Brigham and Women's Hospital), brain, testis, and kidney (Clontech) using Superscript II (GIBCO). Human GAPDHF and GAPDHR were used as a control primer pair.

To examine the alternative splicing variants, we amplified human *PKD1L2* by RT-PCR from human testis cDNA using the primer sets hP7F3 and hP7R4 and hP7F4 and hP7R1. The multiple fragments produced were either extracted and directly sequenced or transformed with a TA TOPO cloning kit (Invitrogen) and examined.

Cell culture

MDCK cells were maintained at 37°C in Dulbecco's modified Eagle's medium (DMEM) containing 5% fetal calf serum, 100 units/ml penicillin, and 100 μg/ml streptomycin. Wild-type $G\alpha_{12}$ or constitutively active $G\alpha_{12}$ (Q229L) stably transfected MDCK cells were grown in DMEM supplemented with 5% fetal calf serum containing 100 units/ml penicillin, 100 μg/ml streptomycin, 100 μg/ml amphotericin, 40 ng/ml doxycycline, 100 μg/ml hygromycin, and 100 μg/ml G418. To induce $G\alpha_{12}$ protein expression, cells were cultured in the absence of doxycycline for 2 days as shown by Meyer et al. [29] and then were lysed in 0.5 ml (per 10-cm dish) of ice-cold lysis buffer (50 mM Tris–HCl, pH 7.6, 150 mM NaCl, 10 mM $MgCl_2$, 1% Triton X-100, 1 mM DTT containing protease inhibitors). The lysates were centrifuged at 10,000*g* at 4°C for 10 min, and the supernatants were subjected to GST pull-down assay and immunoblot analysis.

GST pull-down assay

GST and the GST–polycystin fusion proteins were generated as previously described [25]. In brief, proteins were expressed in the *E. coli* DH5α cells. The bacteria were grown in selective medium containing 2% glucose to an A_{600} of 0.8 at 37°C, followed by induction with 0.1 or 1 mM isopropyl β-D-thiogalactopyranoside (IPTG) at 30°C for another 1 or 2 h. Cells were harvested by centrifugation and resuspended in PBS solution containing 5 mM DTT, 1 mg/ml lysozyme, and protease inhibitors and sonicated on ice. The GST fusion proteins were purified from these cell lysates by binding the fusion proteins to glutathione–Sepharose 4B beads in accordance with the manufacturer's instructions (Amersham Pharmacia Biotech). Wild-type $G\alpha_{12}$ and constitutively active $G\alpha_{12}$ (Q229L)-expressing MDCK cells and untransfected MDCK cell lysates were incubated with GST fusion proteins immobilized on glutathione–Sepharose beads (Amersham Pharmacia Biotech) at 4°C overnight. The beads were centrifuged and were washed five times with 1 ml of ice-cold washing buffer (25 mM Tris–HCl, pH 7.5, 200 mM NaCl, 1 mM $CaCl_2$, 0.5% Triton X-100) after the separation of supernatant as an unbound fraction. The washed beads were solubilized in an equal volume of 2× SDS sample buffer and proteins eluted by incubation at 95°C for 5 min and analyzed by SDS–polyacrylamide gel electrophoresis and Western blotting.

Western blotting

After analysis by SDS–PAGE on 12% polyacrylamide gels, the proteins were transferred onto nitrocellulose membranes (Amersham Pharmacia Biotech). The membranes were blocked with 3 or 5% nonfat dry milk in TBST (Tris-buffered saline containing 0.1% Tween 20) for 30 min and incubated overnight at 4°C with antibody to the $G\alpha_{12}$, $G\alpha_s$, or $G\alpha_{i1-2}$ (Santa Cruz; 1:1000). After three washes with TBST, the membranes were incubated with peroxidase-conjugated goat anti-rabbit IgG (1:5000) for 1 h. Finally the blots were developed by the enhanced chemiluminescence method.

Acknowledgments

We thank Amy Wiebe (Renal Division, Brigham and Women's Hospital), Matthew Sole (Renal Division, Brigham and Women's Hospital), and Eric Williams (Renal Division, Brigham and Women's Hospital) for technical assistance and Sofia Ahmed (Renal Division, Brigham and Women's Hospital) for manuscript preparation. This work was supported by an Uehara Memorial Foundation Research Fellowship to Takeshi Yuasa and by grants from the National Institute of Diabetes, Digestive and Kidney Diseases to Jing Zhou.

References

[1] B.I. Freedman, J.M. Soucie, A. Chapman, J. Krisher, W.M. McClellan, Racial variation in autosomal dominant polycystic kidney disease, Am. J. Kidney Dis. 35 (2000) 35–39.
[2] D.J. Peters, L.A. Sandkuijl, Genetic heterogeneity of polycystic kidney disease in Europe, Contrib. Nephrol. 97 (1992) 128–139.
[3] The International Polycystic Kidney Disease Consortium, Polycystic kidney disease: the complete structure of the PKD1 gene and its protein, Cell 81 (1995) 289–298.
[4] J. Hughes, et al., The polycystic kidney disease 1 (PKD1) gene encodes a novel protein with multiple cell recognition domains, Nat. Genet. 10 (1995) 151–160.
[5] J. Hughes, C.J. Ward, R. Aspinwall, R. Butler, P.C. Harris, Identification of a human homologue of the sea urchin receptor for egg jelly: a polycystic kidney disease-like protein, Hum. Mol. Genet. 8 (1999) 543–549.
[6] T. Yuasa, et al., The sequence, expression, and chromosomal localization of a novel polycystic kidney disease 1-like gene, PKD1L1, in human, Genomics 79 (2002) 376–386.
[7] M.C. Schneider, et al., A gene similar to PKD1 maps to chromosome 4q22: a candidate gene for PKD2, Genomics 38 (1996) 1–4.
[8] T. Mochizuki, et al., PKD2, a gene for polycystic kidney disease that encodes an integral membrane protein, Science 272 (1996) 1339–1342.
[9] H. Nomura, et al., Identification of PKDL, a novel polycystic kidney disease 2-like gene whose murine homologue is deleted in mice with kidney and retinal defects, J. Biol. Chem. 273 (1998) 25967–25973.
[10] G. Wu, et al., Identification of PKD2L, a human PKD2-related gene: tissue-specific expression and mapping to chromosome 10q25, Genomics 54 (1998) 564–568.
[11] L. Guo, et al., Identification and characterization of a novel polycystin family member, polycystin-L2, in mouse and human: sequence, expression, alternative splicing, and chromosomal localization, Genomics 64 (2000) 241–251.
[12] B. Veldhuisen, L. Spruit, H.G. Dauwerse, M.H. Breuning, D.J. Peters, Genes homologous to the autosomal dominant polycystic kidney disease genes (PKD1 and PKD2), Eur. J. Hum. Genet. 7 (1999) 860–872.
[13] S. Gonzalez-Perret, et al., Polycystin-2, the protein mutated in autosomal dominant polycystic kidney disease (ADPKD), is a Ca^{2+}-permeable nonselective cation channel, Proc. Natl. Acad. Sci. USA 98 (2001) 1182–1187.
[14] P.M. Vassilev, et al., Polycystin-2 is a novel cation channel implicated in defective intracellular Ca(2+) homeostasis in polycystic kidney disease, Biochem. Biophys. Res. Commun. 282 (2001) 341–350.
[15] P. Koulen, et al., Polycystin-2 is an intracellular calcium release channel, Nat. Cell Biol. 4 (2002) 191–197.
[16] Y. Luo, P.M. Vassilev, X. Li, Y. Kawanabe, J. Zhou, Native polycystin 2 functions as a plasma membrane Ca^{2+}-permeable cation channel in renal epithelia, Mol. Cell Biol. 23 (2003) 2600–2607.
[17] X.Z. Chen, et al., Polycystin-L is a calcium-regulated cation channel permeable to calcium ions, Nature 401 (1999) 383–386.
[18] N. Nims, D. Vassmer, R.L. Maser, Transmembrane domain analysis of polycystin-1, the product of the polycystic kidney disease-1 (PKD1) gene: evidence for 11 membrane-spanning domains, Biochemistry 42 (2003) 13035–13048.
[19] F. Qian, et al., PKD1 interacts with PKD2 through a probable coiled-coil domain, Nat. Genet. 16 (1997) 179–183.
[20] L. Tsiokas, E. Kim, T. Arnould, V.P. Sukhatme, G. Walz, Homo- and heterodimeric interactions between the gene products of PKD1 and PKD2, Proc. Natl. Acad. Sci. USA 94 (1997) 6965–6970.
[21] A. Guerrero, A. Darszon, Evidence for the activation of two different Ca^{2+} channels during the egg jelly-induced acrosome reaction of sea urchin sperm, J. Biol. Chem. 264 (1989) 19593–19599.

[22] P. Delmas, et al., Constitutive activation of G-proteins by polycystin-1 is antagonized by polycystin-2, J. Biol. Chem. 277 (2002) 11276–11283.
[23] S.M. Nauli, et al., Polycystins 1 and 2 mediate mechanosensation in the primary cilium of kidney cells, Nat. Genet. 33 (2003) 129–137.
[24] E. Kim, et al., Interaction between RGS7 and polycystin, Proc. Natl. Acad. Sci. USA 96 (1999) 6371–6376.
[25] S.C. Parnell, et al., The polycystic kidney disease-1 protein, polycystin-1, binds and activates heterotrimeric G-proteins in vitro, Biochem. Biophys. Res. Commun. 251 (1998) 625–631.
[26] S.C. Parnell, et al., Polycystin-1 activation of c-Jun N-terminal kinase and AP-1 is mediated by heterotrimeric G proteins, J. Biol. Chem. 277 (2002) 19566–19572.
[27] A. Li, X. Tian, S.W. Sung, S. Somlo, Identification of two novel polycystic kidney disease-1-like genes in human and mouse genomes, Genomics 81 (2003) 596–608.
[28] M. Kozak, Interpreting cDNA sequences: some insights from studies on translation, Mamm. Genome. 7 (1996) 563–574.
[29] T.N. Meyer, C. Schwesinger, B.M. Denker, Zonula occludens-1 is a scaffolding protein for signaling molecules. Galpha(12) directly binds to the Src homology 3 domain and regulates paracellular permeability in epithelial cells, J. Biol. Chem. 277 (2002) 24855–24858.
[30] K.J. Mengerink, G.W. Moy, V.D. Vacquier, suREJ3, a polycystin-1 protein, is cleaved at the GPS domain and localizes to the acrosomal region of sea urchin sperm, J. Biol. Chem. 277 (2002) 943–948.
[31] F. Qian, et al., Cleavage of polycystin-1 requires the receptor for egg jelly domain and is disrupted by human autosomal-dominant polycystic kidney disease 1-associated mutations, Proc. Natl. Acad. Sci. USA 99 (2002) 16981–16986.
[32] R.A. Hegele, L. Tu, P.W. Connelly, Human hepatic lipase mutations and polymorphisms, Hum. Mutat. 1 (1992) 320–324.
[33] A. Bateman, R. Sandford, The PLAT domain: a new piece in the PKD1 puzzle, Curr. Biol. 9 (1999) R588–R590.
[34] K. Hanaoka, W.B. Guggino, cAMP regulates cell proliferation and cyst formation in autosomal polycystic kidney disease cells, J. Am. Soc. Nephrol. 11 (2000) 1179–1187.
[35] R. Mangoo-Karim, M. Uchic, C. Lechene, J.J. Grantham, Renal epithelial cyst formation and enlargement in vitro: dependence on cAMP, Proc. Natl. Acad. Sci. USA 86 (1989) 6007–6011.
[36] T. Yamaguchi, et al., Cyclic AMP activates B-Raf and ERK in cyst epithelial cells from autosomal-dominant polycystic kidneys, Kidney Int. 63 (2003) 1983–1994.
[37] T. Eschenhagen, et al., Increased messenger RNA level of the inhibitory G protein alpha subunit Gi alpha-2 in human end-stage heart failure, Circ. Res. 70 (1992) 688–696.
[38] A. Bardaji, et al., Left ventricular mass and diastolic function in normotensive young adults with autosomal dominant polycystic kidney disease, Am. J. Kidney Dis. 32 (1998) 970–975.
[39] U. Belet, et al., Prevalence of epididymal, seminal vesicle, prostate, and testicular cysts in autosomal dominant polycystic kidney disease, Urology 60 (2002) 138–141.
[40] K. Hanaoka, et al., Co-assembly of polycystin-1 and -2 produces unique cation-permeable currents, Nature 408 (2000) 990–994.
[41] M.A. Maw, et al., A third Wilms' tumor locus on chromosome 16q, Cancer Res. 52 (1992) 3094–3098.
[42] S. Grootenboer, et al., Pleiotropic syndrome of dehydrated hereditary stomatocytosis, pseudohyperkalemia, and perinatal edema maps to 16q23–q24, Blood 96 (2000) 2599–2605.
[43] H. Tsuda, D.F. Callen, T. Fukutomi, Y. Nakamura, S. Hirohashi, Allele loss on chromosome 16q24.2–qter occurs frequently in breast cancers irrespective of differences in phenotype and extent of spread, Cancer Res. 54 (1994) 513–517.
[44] H. Suzuki, et al., Three distinct commonly deleted regions of chromosome arm 16q in human primary and metastatic prostate cancers, Genes Chromosomes Cancer 17 (1996) 225–233.
[45] M. Sato, et al., Identification of a 910-kb region of common allelic loss in chromosome bands 16q24.1–q24.2 in human lung cancer, Genes Chromosomes Cancer 22 (1998) 1–8.
[46] Y.H. Chou, K.C. Chung, L.B. Jeng, T.C. Chen, Y.F. Liaw, Frequent allelic loss on chromosomes 4q and 16q associated with human hepatocellular carcinoma in Taiwan, Cancer Lett. 123 (1998) 1–6.
[47] M. Visser, et al., Allelotype of pediatric rhabdomyosarcoma, Oncogene 15 (1997) 1309–1314.
[48] R.D. Page, TreeView: an application to display phylogenetic trees on personal computers, Comput. Appl. Biosci. 12 (1996) 357–358.